Chapter

ZnO Nanowire Field-Effect Transistor for Biosensing: A Review

Nonofo Mathiba Jack Ditshego

Abstract

The last 19 years have seen intense research made on zinc oxide (ZnO) material, mainly due to the ability of converting the natural n-type material into p-type. For a long time, the p-type state was impossible to attain and maintain. This chapter focuses on ways of improving the doped ZnO material which acts as a channel for nanowire field-effect transistor (NWFET) and biosensor. The biosensor has specific binding which is called functionalization that is achieved by attaching a variety of compounds on the designated sensing area. Reference electrodes and buffers are used as controllers. Top-down fabrication processes are preferred over bottom-up because they pave way for mass production. Different growth techniques are reviewed and discussed. Strengths and weaknesses of the FET and sensor are also reviewed.

Keywords: zinc oxide (ZnO), semiconductor device, nanosensor, nanowire field-effect transistor (NWFET), biosensors, growth techniques

1. Introduction

Zinc oxide (ZnO) material has been known as a semiconductor for over 70 years, with some of the first literature being reported as early as in 1944 [1]. It was never put to use like other semiconductors (GaN, Si) because it is difficult to dope. The past 19 years have seen a revival on the research and use of material because of new and emerging ways of doping it. The material is naturally n-type [1–4], and by controlling the conditions of growth, the donor concentration can be controlled. The growth conditions include temperature, diethyl zinc (DEZ) reactant, O_2 or H_2O reactant, and pressure. P-type material [1–4] is difficult to grow and tends to slowly revert back to n-type. Researchers [5–14] who managed to deposit the p-type material have shown that it converts back to n-type within a few days. Maximum time period shown on p-type ZnO was a few months [5–14].

ZnO is a wide bandgap semiconductor [e.g., (0 K) = (3.441 ± 0.003) eV; (300 K) = (3.365 ± 0.005) eV]. It belongs to the group of II^b-VI compound semiconductors which crystalize exclusively in the hexagonal wurtzite-type structure. The lattice parameters of the wurtzite crystal structure are: a = 3.24 Å and c = 5.21 Å. Related to similar II^b-VI (e.g., CbS, CbSe, ZnSe, and ZnS) or III-V (e.g., AlSb, Bas, GaN, and InSb) semiconductors, it has comparatively strong polar binding and large exciton binding energy of (59.5 ± 0.5) meV. Its density is 5.6 g cm^{-3}, a value which corresponds to 4.2×10^{22} ZnO molecules per cm^{-3} [1, 2].

ZnO has practical advantages that make it an attractive semiconductor from an industrial point of view. It has low cost; is abundant, nontoxic, and transparent; has large excitonic binding energy of 60 meV; is soluble, compatible with intercellular material; and has wide and direct bandgap of 3.37 eV, making it highly sensitive. It is well known that semiconductors have a small bandgap which allows switching between conduction and off-states. The larger the bandgap, the better the semiconductor is able to switch states and insulate leakage currents. Bandgap affects sensitivity because a device that possesses a wider bandgap allows for higher currents to travel but also prevents leakage currents, which results in more sensitive and accurate readings. With low-temperature fabrication processes, high-quality devices can be fabricated using the conventional processing technology, thereby making it suitable for low-cost mass-production. It has potential applications in optoelectronics, transparent electronics, and spintronics. ZnO and its alloys have versatile electrical and optical properties for applications in thin film or nanowire transistors, light emitters, biosensors, and solar cells. The nanowire biosensor has a high surface-to-volume ratio, enabling real-time and label-free detection [1–4, 15–17].

Currently, the main commercial application for ZnO (and/or IGZO) material is in displays, with companies like Sharp and Samsung putting IGZO into mobile phone displays [18–20]. IGZO displays outperform other semiconductor displays such as amorphous silicon and organic semiconductors by providing improved resolution and reduced power consumption. This is possible because IGZO has a 20× to 50× times higher mobility than amorphous silicon and polymers, which allows for device scaling without affecting performance [18–20]. Higher mobility values can also be achieved with amorphous silicon technology, but it needs to be laser annealed which is expensive.

2. Growth techniques of ZnO

ZnO films can be grown using three methods: gas transport (vapor phase deposition), hydrothermal synthesis, and/or melt process. Melt growth techniques are a problem due to high vapor pressure of ZnO. Growth using gas transport is difficult to control for large film layers and is normally used for bottom-up ZnO nanostructures. Hydrothermal synthesis is therefore preferred as a method of growth. Thin films can be produced through chemical vapor deposition, metalorganic vapor phase epitaxy, electrodeposition, pulsed laser deposition, sputtering, sol–gel synthesis, atomic layer deposition, spray pyrolysis, etc. All the mentioned techniques fall under hydrothermal synthesis, and one of the preferred methods is atomic layer deposition (ALD). The ALD process is capable of producing highly conformal and quality films [21]. The process is cyclic and is based on the number of reactants. **Figure 1** shows that the ALD process for ZnO films is cyclic and depends on two reactants: metallization and oxidation.

Metallization uses diethyl zinc (DEZ) as the zinc (Zn) metal precursor. Purge and pump steps are used to separate the execution of the reactants and to remove by-products. Before deposition, the wafer (substrate) is preheated at a temperature that will be used for deposition and it is also cleaned with O_2 plasma so as to remove any polymer layer. During the metallization step, the DEZ (Zn $(C_2H_5)_2$) is absorbed onto the surface of the wafer and the residual Zn $(C_2H_5)_2$ is removed from chamber. "R" in **Figure 1** represents C_2H_5.Then on another step, water or O_2 is delivered to react with the absorbed DEZ [23–25]. These steps are executed separately, and to ensure this, purge steps are introduced in between the steps.

When water is used instead of O_2 for oxidation, the process is called thermal ALD. This process tends to produce films similar to chemical vapor deposition (CVD)

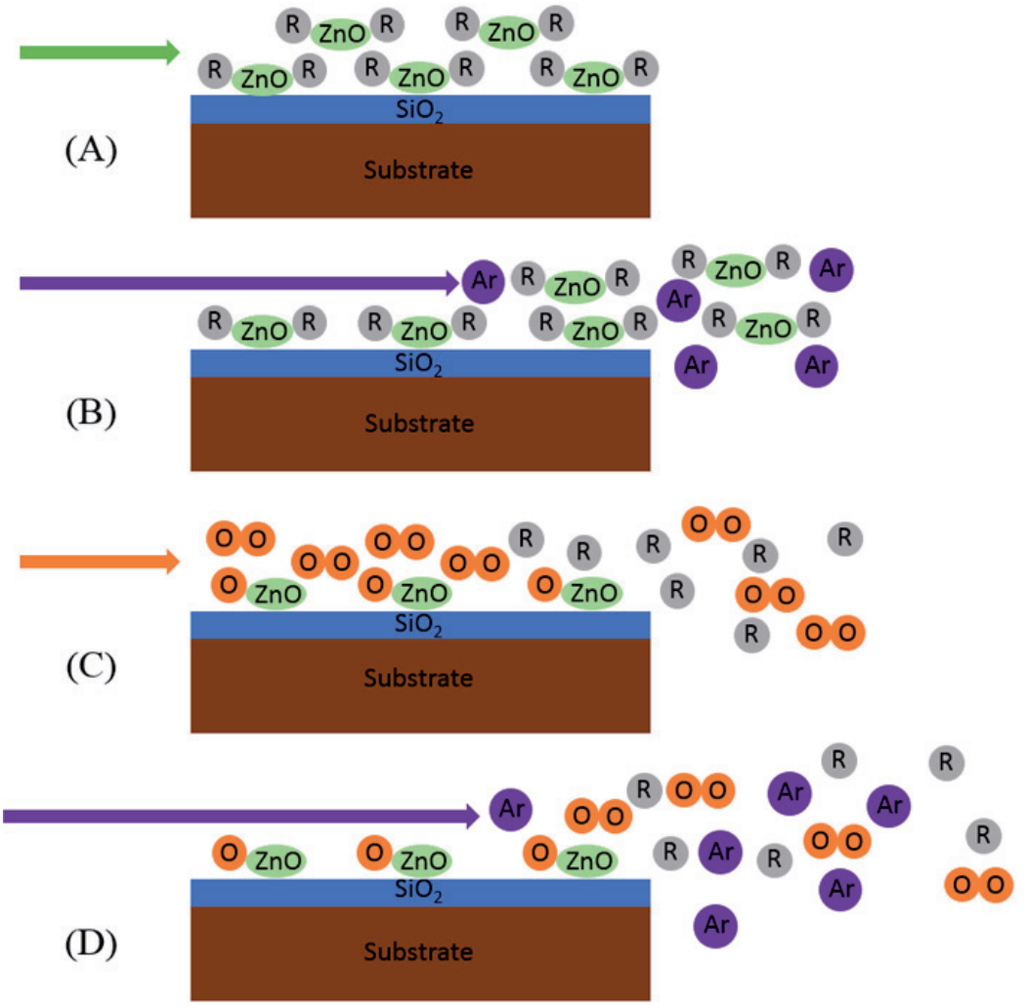

Figure 1.
Schematic diagram illustrating a single cycle of ZnO deposition using the ALD tool (A) metallisation and oxidation step, (B) Purge and pump step (C) Cleaning with O2 plasma step, (D) Removing non-used products with Ar step [22].

techniques [25–27]. When O_2 is used instead of water, then the process needs plasma energy. Remote plasma atomic layer deposition (RPALD) is a fairly new process which is why it is still not in used. It is better than the other deposition techniques as it tends to produce films close to epitaxial layers. The layers are crystalline but tend to be nonuniform to the underlining layer which is why they are not called epitaxial layers. It is a process with great potential for depositing highly conformal and quality films. The process is better than thermal ALD in terms of conformity and quality, but both processes do not generally produce epitaxial layers due to nonuniformity to the underlining substrate. The plasma-assisted ALD method has the following advantages: reduction of OH impurity, allows more freedom in processing conditions, and provides wider range of material properties. The OH impurity is not desired as it affects the conductivity of the semiconductor and induces defects in the dielectrics.

Table 1 compares various growth techniques and how they affect NWFET output characteristics. Chemical vapor deposition (CVD) is the most popular technique for bottom-up nanowire processes. There are two growth techniques classified under CVD which are vapor–liquid–solid (VLS) and vapor–solid (VS) deposition techniques. CVD normally give the highest mobility as they produce crystalline wires with the only flaw being from the catalysts that guide the growth. VS produces better quality nanowires than VLS as it uses no catalysts but instead uses very high temperatures (>900°C). The problem with VS is that it is usually harder to control the size and morphology of the nanowires.

No	Processing route	Synthesis method	Starting materials	Synthesis temp. (°C)	Morphology	Diameter of ZnO nanostructure (mm)	Length of ZnO nanostructure	Ref.
1	Vapor phase processing	Thermal evaporation	Zn metal, O_2, and Ar	650–670	Nanowire	100	Several microns	[29]
2	Route		Zn metal pellets, O_2, Ar	900	Nanowire	20	—	[30]
3			Zn powder, O_2, Ar	600	Nanowire	80	1 μm	[31]
4		Vapor phase transport	ZnO powder, graphite, Cu catalyst	930	Hierarchical dendrite	60–800	—	[32]
5		Aerosol	Zn powder, N_2 gas	500–750	Fiber-mat	100–300	—	[33]
6					Cauliflower	20–30	—	
7		RF sputtering	ZnO deposited over Pt sputtered interdigitated alumina substrate	—	Nanobelt	—	Few micrometer	[34]
8		Molecular beam epitaxy	Zn metal, O_3/O_2 plasma discharge, Au coated substrate	600	Nanorod	50–150	2–10 μm	[35]
9	Solid-state processing	Carbothermal reduction	ZnO powder, graphite powder, Ar gas flow, Au coated silicon substrate	900–925	Nanowire	80–120	10–20 μm	[36, 37]
10	Route	Solid-state Chemical	$ZnCl_2$, NaOH, polyethylene Glycol, $Na_2WO_4.2H_2O$	RT	Nanorod	40–60	200 nm	[38]
11		Reaction				20–40	100 nm	
12	Wet processing	Hydrothermal	$ZnAc^2$, NaOH, absolute ethanol, distilled water	180	Nanorod	—	—	[39]
13	Route		$Zn(CH_3COO)_2{\cdot}2H_2O$, $C_6H_8O_7{\cdot}H_2O$, absolute ethanol, distilled water	400	Nanorod (vertically aligned)	50	500 nm	[40]
14			$Zn(NO_3)_2{\cdot}6H_2O$, NaOH, cetyltrimethyl ammonium bromide, ethanol	120	Nanorod	—	—	[41]

No	Processing route	Synthesis method	Starting materials	Synthesis temp. (°C)	Morphology	Diameter of ZnO nanostructure (mm)	Length of ZnO nanostructure	Ref.
15			$Zn(NO_3)_2{\cdot}6H_2O$, NaOH, cyclohexylamine, ethanol, water	200	Nanorod	150–200	2 μm	[42]
16			$Zn(SO_4){\cdot}7H_2O$, NH_4OH, deionized water	75–95	Nanorod	—	—	[43]
17		ALD	DEZ ($Zn(C_2H_5)_2$), H_2O	—	Nanowire	70–100	5 μm	[44]
18		Plasma ALD	DEZ ($Zn(C_2H_5)_2$), O_2	150–190	Nanowire	36–100	2–20 μm	[22]

Table 1.
Summary of various methods used for the production of 1-D ZnO nanostructures, adopted from [28].

Table 1 also shows that atomic layer deposition (ALD) is an attractive technique because it deposits high quality films at low temperatures between 120 and 210°C [22, 45]. The problem with ALD is that it has only this window for good quality conducting films. At temperatures below 120°C, the deposition can be incomplete or experience condensation depending on growth rate. At temperatures above 210°C, the deposition tends to experience desorption or it decomposes toward CVD deposition. Nonetheless, it is one of the best techniques toward growing films close to epitaxial growth (crystallinity is achievable whereas uniformity is still difficult to achieve) [22, 45]. The tool has shown potential by achieving high values of field effect mobility >30 cm^2/Vs with excellent crystallinity.

2.1 Native point defects

There are three types of defects in a crystal lattice: point defects, area defects, and volume defects. Point defects which are caused by native elements and impurities are the major problem for ZnO semiconductor. Native point defects for ZnO include the following: zinc interstitial (Zn_i), zinc antisite (Zn_o), zinc vacancy (V_{Zn}), oxygen interstitial (O_i), oxygen antisite (O_{Zn}), and oxygen vacancy (V_o). Over the years, a lot of research advocated them as the major cause for the n-type behavior. Oxygen defects are seen as the main contributors toward the n-type behavior [3, 15]. There are some researchers [1–4] who hypothesize that impurities (not the native point defects) are the main cause of the n-type behavior because they tend to be shallow donors whereas Zn and O_2 defects tend to be deep donors [1–4]. The two theories have not been proven so currently the main cause of the natural n-type behavior of ZnO [1–4] is not certain.

2.2 Deep donors versus shallow donors: ZnO

ZnO impurities (foreign atoms) are normally incorporated in the crystal structure of the semiconductor. There are two reasons of impurity incorporation: they can either be unintentionally introduced due to lack of control during growth processes or they are intentionally added to increase the number of free carriers in the semiconductor. Impurities in the ZnO should have the ability to be ionized; which is desirable as it increases conductivity. This means that the impurity atoms should be able to give off electrons to the conduction band. If the impurities were acceptors—they should be able to give off holes to the valence band [3, 16].

Donor Impurities for the n-type ZnO can either be shallow or deep. **Figure 2** shows shallow donors compared to deep donors. Shallow impurities require little energy to ionize (this is energy typically around the thermal energy or less). These donor impurities possess energy close to the band edge—the extra valence electron

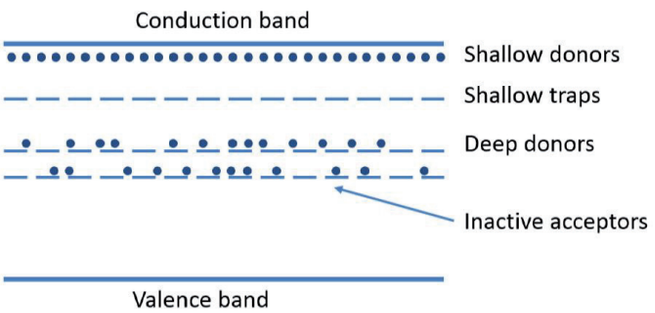

Figure 2.
Shallow versus deep donors [1–4].

of these impurities are loosely bound and occupy effective-mass states near the conduction band maximum- CBM- at low temperatures. Deep impurities on-the-other-hand require energy greater that the thermal energy to ionize. These donor impurities possess energy far from the band edge (CBM) making them very hard to ionize. Their presence within the semiconductor tends to contribute only a small fraction of free carriers. Deep donors are also called traps because they act as effective recombination centers in which electrons and holes fall and annihilate each other. Grain boundaries (GB) are main source of deep state impurities and they adversely affect transistor performance. ZnO is a wide bandgap material and research suggests [3, 4, 16] that there exist possible deep-level traps in GBs. The examples of deep donors are Zn and O ions. Zn acts as a deep donor when there is a vacancy and O acts as a deep donor in any defect state. An example of a shallow donor is the H ion.

2.3 Top-down fabrication of ZnO nanowire FETs

There are four main methods capable of producing nanometer features using top-down approaches: UV stepper lithography, e-beam lithography [46], focused ion-beam lithography [47], and spacer method [45, 48]. UV lithography is the standard industrial method for fabricating nanodevices. E-beam and focused ion-beam lithography are often used and can pattern devices down to 5 nm, but the equipment is very expensive and the pattern writing is very slow. These two instruments resemble scanning electron microscope (SEM) in terms of operation. Whereas SEM is used to focus a beam of electrons to image samples within a chamber, these instruments are used to create patterns on the samples. The difference between e-beam and focused ion-beam is that the latter uses an ion beam to pattern wafers and hence does not require photoresist. Their advantage over optical UV lithography is the small features they reach. For low-cost applications such as biosensors, the problem with these two methods is that they are expensive.

The spacer technique is a low-cost fabrication method for fabricating nanowires. It was first reported in 2005 by Ge et al. [49], and other researchers [44, 50, 51] have since carried it forward. The technique has great potential in shaping nanometer features using conventional, low-cost photolithography. **Figure 3** shows the concept of the spacer technique. It uses first anisotropic etch to create a vertical pillar on an insulating layer (SiO_2), then after deposition of a semiconductor layer (ZnO) and a second anisotropic etch, to create nanowires made up of the semiconductor layer. This method allows nanowire features with controllable dimensions to be developed. The ICP tool is usually used for anisotropic etching and produces

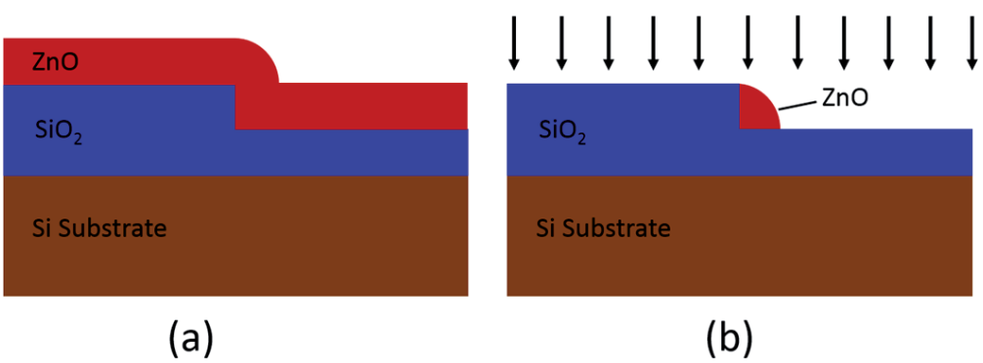

Figure 3.
Novel spacer technique used to pattern nanowire features. Cross-sectional schematic of nanowire formation (a) before dry etch and (b) after dry etch [22].

surface roughness <1.5 nm. Other tools such as RIE and ion beam etch produce roughness >5 nm. The fabrication process for the complete ZnO NWFET structure is as outlined in [52].

3. Background on FETs

The ZnO field-effect transistor (FET) has been around for decades. The success of the device in meeting the technological demands has largely been dominated by the shrinking size of its physical geometry. It has an advantage as a junctionless (no p-n junctions) FET compared to conventional FETs [17, 21, 23–27, 53, 54]. There has been an introduction of new materials and heterojunction structures developed so as to move away from conventional silicon devices. High-K dielectrics have been introduced to replace the conventional SiO_2 which should help maintain acceptable dielectric thicknesses while keeping gate leakage currents low [17, 21, 23–27, 53, 54].

Even with so many improvements being made to the device, the limits of FET scaling are approaching. The thickness of the oxide (t_{ox}) cannot be less than 1 nm due to high tunneling current and significant operational variation. The substrate doping is also very high which creates leakage and tunneling currents that are unacceptable to device operation.

3.1 ZnO thin film transistors (TFTs)

TFTs have also been fabricated using ZnO, mainly as thin film transistors for application in displays. **Figure 4** compares 20 ZnO TFTs fabricated by different authors [27, 53–71] using a variety of fabrication methods over the last 5 years. The graph is a plot of field effect mobility versus subthreshold slope which are two of the main parameters that describe the performance and efficiency of a device. The best device was fabricated by Bayraktaroglu et al. [70] with a SiO_2 insulator and pulsed laser-deposited ZnO active channel layer. The device had a field effect mobility 110 cm^2/Vs and an excellent subthreshold gate voltage swing of 109 mV/decade. This value of mobility is much higher than the value of around 1 cm^2/Vs that is typically achieved with amorphous silicon TFTs in production displays. It is clear therefore that ZnO TFTs have considerable potential for application in high performance displays.

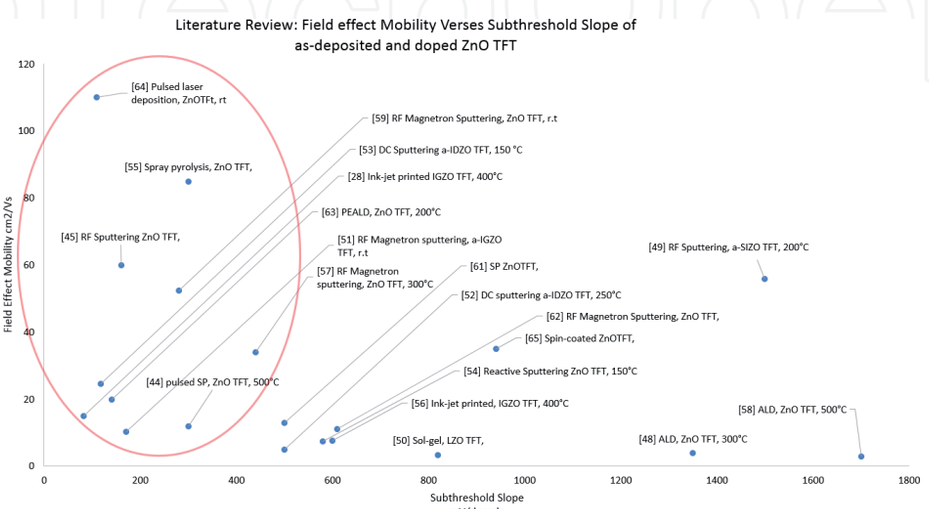

Figure 4.
General literature review on TFTs looking at field effect mobility versus subthreshold slope of as-deposited and doped ZnO films.

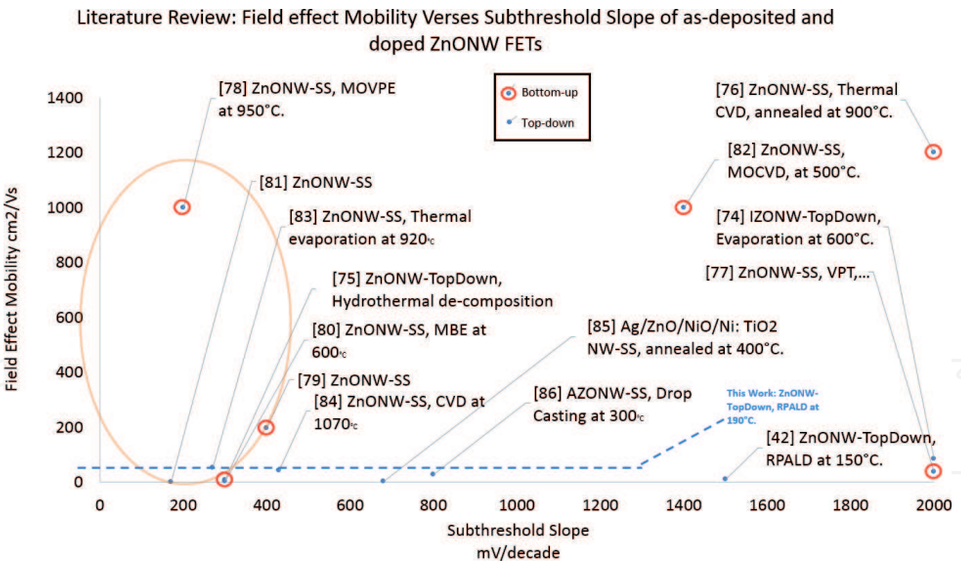

Figure 5.
Literature review on nanowire FETs looking at field effect mobility versus subthreshold slope of as-deposited and doped ZnO nanowires.

3.2 Nanowire field-effect transistors (FETs)

Emerging nonplanar devices [17, 21] are being researched to prolong the future progress for FETs. Devices based on quasi-one-dimensional (1-D) nanostructures are still at an embryonic stage from an industrial point of view. These nanostructures include the following: nanowires, nanobelts, nanoribbons, and nanoneedles [72, 73]. This review is interested in nanowire FETs which are also being researched for application in biosensors because the high surface-to-volume ratio provides high sensitivity.

3.3 Comparing ZnO NWFETs

Figure 5 compares 15 different ZnO NWFETs fabricated by different authors using a variety of methods [22, 74–86]. The graph is plotted with field effect mobility against the subthreshold slope, which are two important device parameters that determine ZnO NWFET performance. The nanowires were fabricated using top-down and bottom-up (self-assembled) processes. Self-assembled processes tend to display very high field effect mobility which is normally above 200 cm^2/Vs; whereas the top-down have lower mobility values. Most of the top-down fabricated devices have mobility <1.0 cm^2/Vs with around three papers giving a mobility >10.0 cm^2/Vs. The difference in the mobility may be due to the fact that self-assembled nanowires are single-crystal, whereas top-down nanowires are polycrystalline. Nonetheless, top-down techniques are desirable as they currently pave way for mass production and will be pursued in this research investigation.

4. Biosensors

A biosensor is defined by the International Union of Pure and Applied Chemistry (IUPAC) as "a self-contained integrated device that is capable of providing specific quantitative or semiquantitative analytical information using a biological recognition element (biochemical receptor), which is retained in contact direct with a transduction element" [87]. A biosensor is a "more-than-Moore device" because it

incorporates functionalities that do not necessarily scale according to Moore's law. Under the roadmap, the device falls under the category of sensors and actuators. Other categories include analogue/RF, passives, HV power, and biochips [88, 89].

Figure 6 shows a typical structure of a biosensor [90–92]. The biomolecules are contained within an analytic solution and attach themselves to immobilized enzymes or immune-agents on the linkers. Linkers in turn are attached to the transducer. The transducer then converts the charge on the analyte into an electrical signal which is then transmitted for data processing. Biosensors can be considered as part of the research field known as "chemical sensors" in that a biological mechanism is used for analyte detection within an analyte solution [93–95]. Quasi-one-dimensional nanostructures have a greater surface-to-volume ratio compared to planar structures and are therefore expected to be more sensitive than planar sensors [93–95].

Nanowires are the same as nanorods. The words can be used interchangeably [80]. These have received enormous attention due to their suitable properties for designing novel nanoscale biosensors. For example, the dimensions of ~1–100 nm are similar to those of many biological entities, such as nucleic acids, proteins, viruses, and cells [79]. In addition, the high surface-to-volume ratios for nanomaterials allow a large proportion of atoms in the bio-analyte to be located at or close to the surface. Moreover, some nanowire materials have surfaces that can easily be chemically

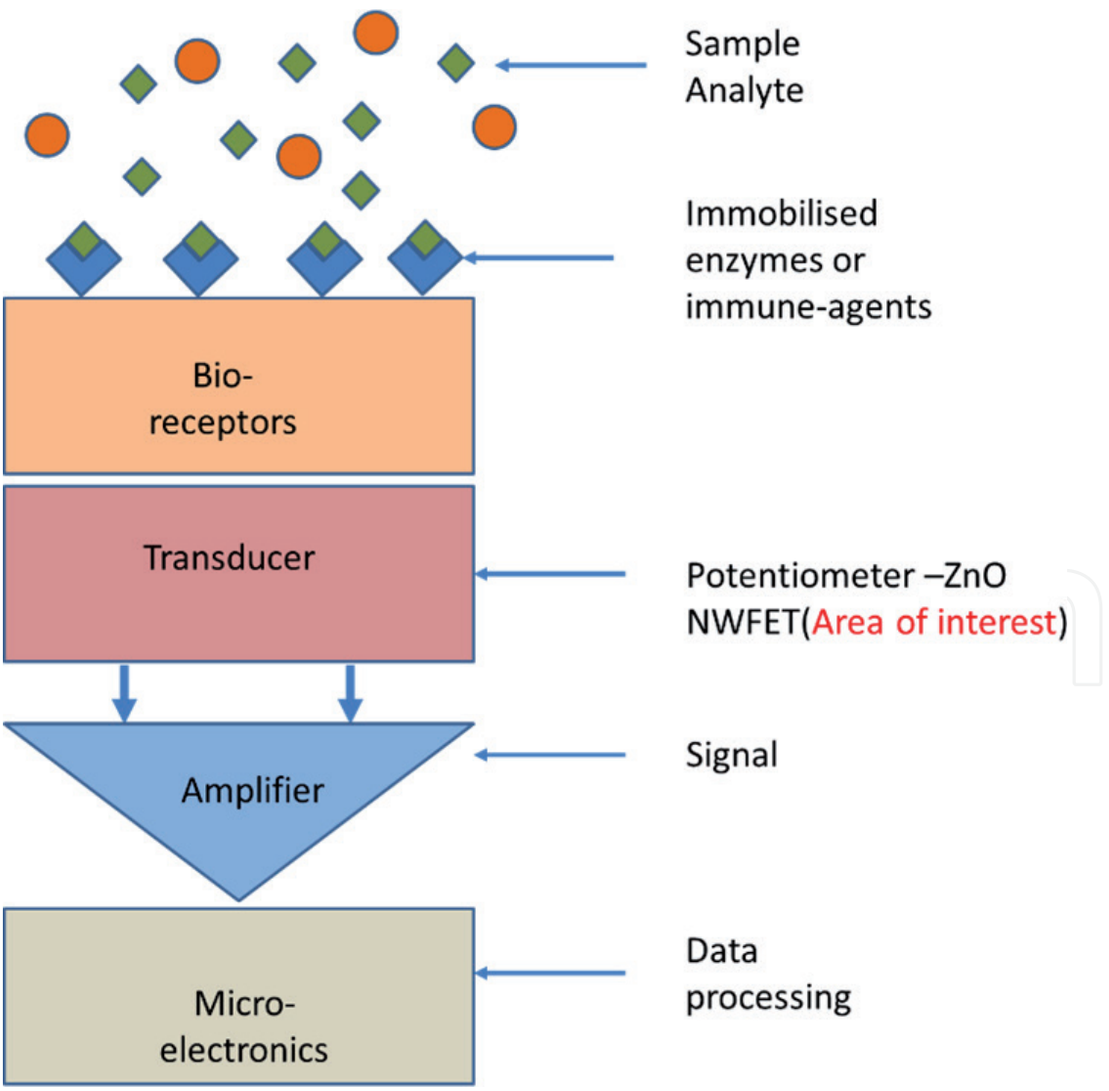

Figure 6.
Typical structure of a biosensor. The biomolecules are contained within an analytic solution and attach themselves to immobilized enzymes or immune-agents on the receptors. The transducer then converts the energy signal produced into an electrical signal which is then transmitted for data processing. [22].

modified which makes them significant candidates for biosensors [79, 80]. There are a number of nanostructure-based electrical biosensors which include single-wall carbon nanotubes (SWCNT), nanowires, nanogaps, nanochannels, and nano-electromechanical (NEM) devices. The project will focus on nanowire-based devices as they have considerable potential for electrical biosensing that offer the possibility of portable assays in a variety of point-of-care environments [48, 90, 96].

4.1 Silicon biosensors

Over the past decade, silicon nanowires have been the most researched for application as biochemical sensors [97–108]. Silicon nanowires are of interest for a number of reasons, for example, the material is well known and is compatible with CMOS integrated circuits for the development of sensor systems [97–108]. The nanowire is expected to have high surface-to-volume ratios which give high sensitivity and the electrical sensing will give real-time label-free detection without the use of expensive optical components. Mass manufacturing is also a main advantage for silicon and is critically important for nanowire biosensor applications because of the widespread uptake of biosensors in "point-of-care" settings, the biosensor needs to be disposable [97–108].

A number of fabrication methods are well established for silicon nanowires which utilize both bottom-up and top-down methods (these methods are called hybrids). It still remains that bottom-up techniques have the advantage of simplicity [97–108]. Bottom-up methods are still limited due to the alignment problem. The hybrid methods require further nanowire technologies to achieve alignment, such as electric field or fluid-flow-assisted nanowire positioning to locate the nanowires between lithographically defined source and drain electrodes. The technique is interpreted as a hybrid between bottom-up and top-down. Top-down methods overcome these problems, and several researchers have used advanced lithography techniques to fabricate single-crystal silicon nanowires on silicon-on-insulator (SOI) substrates. SOI wafers are expensive and to overcome the problem some researchers [109] have devised alternatives to SOI. The electrical output characteristics of silicon nanowires are good and they are well suited for biosensing applications. The sensitivity range for most silicon-nanowire based biosensors is between 50 and 400 mV [97–134].

4.2 Comparing ZnO nanowire biosensors

ZnO is investigated as it is expected to be more sensitive than Si due to its wider bandgap [109]. This is observed by comparing **Table 2** with **Table 3**. ZnO devices show results comparable to silicon devices; especially looking at response time and limit of detection. It is required that biosensors should have the liquid reference electrode. There are many different types of ZnO nanostructures being used for sensing application and **Table 2** compares the ZnO nanostructures such as nanotetrapods, nanocombs, and nanorods used for biosensing [110, 121]. Nanotetrapods [123] are like nanorods but with four single crystalline legs. Most of the ZnO devices were synthesized by vapor phase method and then transferred on Au electrode to form a multiterminal network for the sensor receptors. Like all other bottom-up ZnO nanostructures discussed here, they are transferred to a surface of a working electrode to form a thin layer to modify the transducer. The devices have low sensitivity but the nanotetrapods exhibit good detection limit down to ~1.0 nM. The researchers [123] did not explain why the nanostructures possess low sensitivity but its three-dimensional features have the potential for multiterminal communication applications [123].

No.	Reference electrode	Type of sensor	Channel material	ZnO fabrication process	LOD (μM)	Response time (s)	Ref.
1	Au	Biosensor	ZnO nanorod array	Hydrothermal	10	<5	[111]
2	ITO	Biosensor	ZnO nanotube array	Hydrothermal/ chemical	10	<6	[112]
3	Au	Biosensor	Tetrapod-like ZnO	CVD	4	6	[113]
4	Glass capillary	Biosensor	ZnO nanoflakes	Hydrothermal	0.5	<4	[114]
5	GCE	Biosensor	Fork-like ZnO	Annealing	0.3	3	[115]
6	Au	Biosensor	Comb-like ZnO	CVD	20	<10	[116]
7	Ti	Biosensor	ZnO/C nanorod array	Hydrothermal	1	4	[117]
8	ITO	Biosensor	ZnO/ Cu array matrix	Hydrothermal	40	<6	[118]
9	GCE	Biosensor	ZnO/Au nanorods	Hydrothermal	0.01	<5	[119]
10	Pt	Biosensor	ZnO/NiO nanorods	Hydrothermal	2.5	<5	[120]

Table 2.
Summary of characteristics for various 1-D ZnO biosensors, adopted from [110].

No.	Reference electrode	Type of sensor	Channel material	ZnO fabrication process	LOD (pM)	Response time (s)	Ref.
1	No reference electrode	Biosensor	Si NW	nanocluster-mediated vapor–liquid–solid growth method	10	<10	[97]
2	Au	Biosensor	Si NW	Chemical vapor deposition	0.002	<10	[98]
3	Platinum wire	Biosensor	Si NW	SNAP technique	10	<10	[101]
4	None	Biosensor	Si NW	Reactive-ion etching (RIE)	0.01	<10	[106]
5	None	Biosensor	Si NW	Synthesized by chemical vapor deposition	100	<10	[122]

Table 3.
Summary of characteristics for various 1-D Si biosensors, adopted from [121].

In nanocombs [116] design, each comb has between 3 and 10 rods connected to one another by a single rod. ZnO nanocombs were used as the channel for sensing glucose [116] and as label-free uric acid biosensor based on uricase [124]. The functionalized

ZnO nanorods showed thermal stability, anti-interference capability, and direct electron transfer (DET) between enzyme electroactive sites and external electrodes. The activity of the enzyme and the sensitivity can be increased by introducing a lipid film between the channel and the enzyme. Another uric acid biosensor [125] example is based on uricase-functionalized ZnO nanoflakes, which was hydrothermally prepared at low temperatures on Au-coated glass. The sensor produced a sensitivity based on subthreshold slope of ~66 mV/decade. Bottom-up ZnO nanorods [126] were also used as lactate oxidase (LOD) biosensor using glutaraldehyde cross-linkers. The device had a subthreshold sensitivity of ~41 mV/decade, with maximum detection of 0.1 μM. To test for cholesterol, porous ZnO mirco-tubes [127] were constructed using 3-D assembled porous flakes. ZnO nanorods [128] were grown on Ag electrode to make a cholesterol sensor.

5. Conclusion

Most researchers use bottom-up approaches to fabricate the ZnO biosensors because of the straightforward synthesis process. However, these bottom-up devices have variable electrical performance due to the lack of geometrical dimension control and addressing the nanostructures for sensing application. So far, there is limited research reported on top-down ZnO biosensors, and previous work demonstrated the viability of top-down ZnO NWFET for biosensor applications. In the work, however, there was no passivation layer on the ZnO nanowires, which led to the dissolution of the material. This made the device unstable and the sensing results were not reproducible. There exists a need to develop a passivating layer technology and optimize the fabrication process for biosensor applications. That way, a reliable measurement of sensitivity for the nonspecific and specific sensing of lysozyme and bovine serum albumin (BSA) can be achieved.

Acknowledgements

N.M.J. Ditshego would like to acknowledge the Botswana International University of Science and Technology (BIUST) for supporting his doctoral studies and the Southampton Nanofabrication Centre for the experimental work. The author would like to acknowledge the EPSRC EP/K502327/1 grant support.

Author details

Nonofo Mathiba Jack Ditshego
Electrical, Computer and Telecommunications Engineering Department, CET, Botswana International University of Science and Technology (BIUST), Palapye, Botswana

*Address all correspondence to: ditshegon@biust.ac.bw

References

[1] Klingshirn C, Fallert J, Zhou H, Sartor J, Thiele C, Maier-Flaig F, et al. 65 years of ZnO research—old and very recent results. Physica Status Solidi. 2010;**247**(6):1424-1447

[2] Özgür U, Alivov YI, Liu C, Teke A, Reshchikov MA, Doğan S, et al. A comprehensive review of ZnO materials and devices. Journal of Applied Physics. 2005;**98**(4):041301

[3] McCluskey MD, Jokela SJ. Defects in ZnO. Journal of Applied Physics. 2009;**106**(7):071101

[4] Janotti A, Van de Walle CG. Fundamentals of zinc oxide as a semiconductor. Reports on Progress in Physics. 2009;**72**(12):126501

[5] Wang G, Chu S, Zhan N, Zhou H, Liu J. Synthesis and characterization of Ag-doped p-type ZnO nanowires. Applied Physics A: Materials Science & Processing. 2011;**103**(4):951-954

[6] Tsukazaki A, Ohtomo A, Onuma T, Ohtani M, Makino T, Sumiya M, et al. Repeated temperature modulation epitaxy for p-type doping and light-emitting diode based on ZnO. Nature Materials. 2005;**4**(1):42-46

[7] Oh MS, Hwang DK, Lee K, Im S, Yi S. Low voltage complementary thin-film transistor inverters with pentacene-ZnO hybrid channels on Al Ox dielectric. Applied Physics Letters. 2007;**90**(17):173511-173513

[8] Choi J-H, Lee SW, Kar JP, Das SN, Jeon J, Moon K-J, et al. Random network transistor arrays of embedded ZnO nanorods in ion-gel gate dielectric. Journal of Materials Chemistry. 2010;**20**(35):7393

[9] Dunlop L, Kursumovic A, MacManus-Driscoll JL. Reproducible growth of p-type ZnO:N using a modified atomic layer deposition process combined with dark annealing. Applied Physics Letters. 2008;**93**(17):172111

[10] Huang J, Chu S, Kong J, Zhang L, Schwarz CM, Wang G, et al. ZnO p-n homojunction random laser diode based on nitrogen-doped nanowires. Advanced Optical Materials. 2013;**1**(2):179-185

[11] Kumar M, Kar JP, Kim IS, Choi SY, Myoung JM. Fabrication of As-doped p-type ZnO thin film and ZnO nanowire inserted p-n homojunction structure. Applied Physics A: Materials Science & Processing. 2009;**97**(3):689-692

[12] Yuan GD, Zhang WJ, Jie JS, Fan X, Zapien JA, Leung YH, et al. p-type ZnO nanowire arrays. Nano Letters. 2008;**8**(8):2591-2597

[13] Cha SN, Jang JE, Choi Y, Amaratunga GAJ, Ho GW, Welland ME, et al. High performance ZnO nanowire field effect transistor using self-aligned nanogap gate electrodes. Applied Physics Letters. 2006;**89**(26)

[14] Li FM, Hsieh G-W, Dalal S, Newton MC, Stott JE, Hiralal P, et al. Zinc oxide nanostructures and high electron mobility Nanocomposite thin film transistors. IEEE Transactions on Electron Devices. 2008;**55**(11):3001-3011

[15] Murphy TE, Blaszczak JO, Moazzami K, Bowen WE, Phillips JD. Properties of electrical contacts on bulk and epitaxial n-type ZnO. Journal of Electronic Materials. 2005;**34**(4):389-394

[16] Lee D-J, Kwon J-Y, Kim S-H, Kim H-M, Kim K-B. Effect of Al distribution on carrier generation of atomic layer

deposited Al-doped ZnO films. Journal of the Electrochemical Society. 2011;**158**(5):D277

[17] ZnO Devices and Applications: A Review of Current Status and Future Prospects, IEEE Xplore, Proceedings of the IEEE. August 2010;**98**(7):1255-1268. DOI: 10.1109/JPROC.2010.2044550

[18] Triggs R. Display Technology Explained: A-Si, LTPS, Amorphous IGZO, and Beyond (Android Authority). 2014. Available from: http://www.androidauthority.com/amorphous-igzo-and-beyond-399778/ [Accessed: 01 March 2015]

[19] Hruska J. The Perils and Promise of High-Resolution Displays (Extreme Tech) [Online]. 2012. Available from: http://www.extremetech.com/electronics/126519-the-perils-and-promise-of-high-resolution-displays [Accessed: 01 March 2015]

[20] Anthony S. IGZO Display Tech Finally makes it to Mass Market: iPad Air Now, High-res Desktop Display Soon (Extreme Tech) [Online]. 2013. Available from: http://www.extremetech.com/computing/170970-igzo-display-tech-finally-makes-it-to-mass-market-ipad-air-now-high-res-laptops-and-desktops-next [Accessed: 01 March 2015]

[21] Riyadi MA, Suseno JE, Ismail R. The future of non-planar nanoelectronics MOSFET devices: A review. Journal of Applied Sciences. 2010;**10**(18):2136-2146

[22] Sultan SSM. Top-down fabrication and characterization of zinc oxide nanowire field effect transistors [PhD thesis]. University of Southampton; 2013

[23] Park J-S. The annealing effect on properties of ZnO thin film transistors with Ti/Pt source-drain contact. Journal of Electroceramics. 2010;**25**(2-4):145-149

[24] Engineering E. Amorphous In-Ga-Zn-O Thin Film Transistor for Future Optoelectronics by Tze-Ching Fung. 2010

[25] Moon Y, Lee S, Kim D. Characteristics of ZnO based TFT using La2O3 high-k dielectrics. Journal of Korean. 2009;**55**(5):1906-1909

[26] Park SY, Kim BJ, Kim K, Kang MS, Lim KH, Il Lee T, et al. Low-temperature, solution-processed and alkali metal doped ZnO for high-performance thin-film transistors. Advanced Materials. 2012;**24**(6):834-838

[27] Ortel M, Wagner V. Leidenfrost temperature related CVD-like growth mechanism in ZnO-TFTs deposited by pulsed spray pyrolysis. Journal of Crystal Growth. 2013;**363**:185-189

[28] Arafat MM, Dinan B, Akbar SA, Haseeb ASMA. Gas sensors based on one dimensional nanostructured metal-oxides: A review. Sensors (Switzerland). 2012;**12**(6):7207-7258

[29] Lupan O, Ursaki VV, Chai G, Chow L, Emelchenko GA, Tiginyanu IM, et al. Selective hydrogen gas nanosensor using individual ZnO nanowire with fast response at room temperature. Sensors and Actuators B: Chemical. 2010;**144**(1):56-66

[30] Wan Q, Lin CL, Yu XB, Wang TH. Room-temperature hydrogen storage characteristics of ZnO nanowires. Applied Physics Letters. 2004;**84**(1):124

[31] Dong K-Y, Choi J-K, Hwang I-S, Lee J-W, Kang BH, Ham D-J, et al. Enhanced H2S sensing characteristics of Pt doped SnO2 nanofibers sensors with micro heater. Sensors and Actuators B: Chemical. 2011;**157**(1):154-161

[32] Zhang N, Yu K, Li Q, Zhu ZQ, Wan Q. Room-temperature high-sensitivity H[sub 2]S gas sensor based on dendritic ZnO nanostructures with macroscale in appearance. Journal of Applied Physics. 2008;**103**(10):104305

[33] Baratto C, Sberveglieri G, Onischuk A, Caruso B, di Stasio S. Low temperature selective NO2 sensors by nanostructured fibres of ZnO. Sensors and Actuators B: Chemical. 2004;**100**(1-2):261-265

[34] Sadek AZ, Choopun S, Wlodarski W, Ippolito SJ, Kalantar-zadeh K. Characterization of ZnO nanobelt-based gas sensor for H_2, NO_2 and hydrocarbon sensing. IEEE Sensors Journal. 2007;**7**(6):919-924

[35] Wang HT, Kang BS, Ren F, Tien LC, Sadik PW, Norton DP, et al. Hydrogen-selective sensing at room temperature with ZnO nanorods. Applied Physics Letters. 2005;**86**(24):243503

[36] Huang MH, Wu Y, Feick H, Tran N, Weber E, Yang P. Catalytic growth of zinc oxide nanowires by vapor transport. Advanced Materials. 2001;**13**(2):113-116

[37] Ahn M-W, Park K-S, Heo J-H, Park J-G, Kim D-W, Choi KJ, et al. Gas sensing properties of defect-controlled ZnO-nanowire gas sensor. Applied Physics Letters. 2008;**93**(26):263103

[38] Cao Y, Hu P, Pan W, Huang Y, Jia D. Methanal and xylene sensors based on ZnO nanoparticles and nanorods prepared by room-temperature solid-state chemical reaction. Sensors and Actuators B: Chemical. 2008;**134**(2):462-466

[39] Wang C, Chu X, Wu M. Detection of H2S down to ppb levels at room temperature using sensors based on ZnO nanorods. Sensors and Actuators B: Chemical. 2006;**113**(1):320-323

[40] Yang Z, Li L-M, Wan Q, Liu Q-H, Wang T-H. High-performance ethanol sensing based on an aligned assembly of ZnO nanorods. Sensors and Actuators B: Chemical. 2008;**135**(1):57-60

[41] Zhou X, Li J, Ma M, Xue Q. Effect of ethanol gas on the electrical properties of ZnO nanorods. Physica E: Low-dimensional Systems and Nanostructures. 2011;**43**(5):1056-1060

[42] Cho P-S, Kim K-W, Lee J-H. NO2 sensing characteristics of ZnO nanorods prepared by hydrothermal method. Journal of Electroceramics. 2006;**17**(2-4):975-978

[43] Lupan O, Chai G, Chow L. Novel hydrogen gas sensor based on single ZnO nanorod. Microelectronic Engineering. 2008;**85**(11):2220-2225

[44] Ra H-W, Choi K-S, Kim J-H, Hahn Y-B, Im Y-H. Fabrication of ZnO nanowires using nanoscale spacer lithography for gas sensors. Small. 2008;**4**(8):1105-1109

[45] Sultan SM, Ditshego NJ, Gunn R, Ashburn P, Chong HM. Effect of atomic layer deposition temperature on the performance of top-down ZnO nanowire transistors. Nanoscale Research Letters. 2014;**9**(1):517

[46] Donthu S, Pan Z, Myers B, Shekhawat G, Wu N, Dravid V. Facile scheme for fabricating solid-state nanostructures using e-beam lithography and solution precursors. Nano Letters. 2005;**5**(9):1710-1715

[47] Ming L, Hai-Ying Z, Chang-Xin G, Jing-Bo X, Xiao-Jun F. The research on suspended ZnO nanowire field-effect transistor. Chinese Physics B. 2009;**18**(4):1594-1597

[48] Hakim MMA, Lombardini M, Sun K, Giustiniano F, Roach PL, Davies DE, et al. Thin film polycrystalline silicon nanowire

biosensors. Nano Letters. 2012;**12**(4):1868-1872

[49] Ge H, Wu W, Li Z, Jung G-Y, Olynick D, Chen Y, et al. Cross-linked polymer replica of a nanoimprint mold at 30 nm half-pitch. Nano Letters. 2005;**5**(1):179-182

[50] Weber T, Käsebier T, Szeghalmi A, Knez M, Kley E-B, Tünnermann A. Iridium wire grid polarizer fabricated using atomic layer deposition. Nanoscale Research Letters. 2011. Available from: http://www.researchgate.net/profile/Mato_Knez/publication/51738965_Iridium_wire_grid_polarizer_fabricated_using_atomic_layer_deposition/links/0fcfd511134d1c51b7000000.pdf [Accessed: 26 May 2015]

[51] Liu X, Deng X, Sciortino P, Buonanno M, Walters F, Varghese R, et al. Large area, 38 nm half-pitch grating fabrication by using atomic spacer lithography from aluminum wire grids. Nano Letters. 2006;**6**(12):2723-2727

[52] Ditshego NMJ, Sultan SM. Top-down fabrication process of ZnO NWFETs. Journal of Nano Research. 2019;**57**:77-92

[53] Ye Z, Wong M. Characteristics of thin-film transistors fabricated on fluorinated zinc oxide. IEEE Electron Device Letters. 2012;**33**(4):549-551

[54] Yang J, Park JK, Kim S, Choi W, Lee S, Kim H. Atomic-layer-deposited ZnO thin-film transistors with various gate dielectrics. Physica Status Solidi (A) - Applications and Materials Science. 2012;**209**(10):2087-2090

[55] Chong E, Kim B, Lee S. Reduction of channel resistance in amorphous oxide thin-film transistors with buried layer. IOP Conference Series: Materials Science and Engineering. 2012;**34**:012005

[56] Su B, Chu S, Juang Y. Improved electrical and thermal stability of solution-processed Li-doped ZnO thin-film transistors. IEEE Electron Device Letters. 2012;**59**(3):700-704

[57] Choi K, Jeon S, Kim H. A comparison of Ga: ZnO and Ga: ZnO/Ag/Ga: ZnO source/drain electrodes for In–Ga–Zn–O thin film transistors. Materials Research Bulletin. 2012;**47**(10):2915-2918

[58] Chen R, Zhou W, Zhang M. Self-aligned indium–gallium–zinc oxide thin-film transistor with phosphorus-doped source/drain regions. IEEE Electron Device Letters. 2012;**33**(8):1150-1152

[59] Geng D, Kang D. High-speed and low-voltage-driven shift register with self-aligned coplanar a-IGZO TFTs. IEEE Electron Device Letters. 2012;**33**(7):1012-1014

[60] Li S, Cai Y, Han D, Wang Y. Low-temperature ZnO TFTs fabricated by reactive sputtering of metallic zinc target. Electron Devices. 2012;**59**(9):2555-2558

[61] Adamopoulos G, Thomas S, Woebkenberg PH, Bradley DDC, McLachlan MA, Anthopoulos TD. High-mobility low-voltage ZnO and Li-doped ZnO transistors based on ZrO_2 high-k dielectric grown by spray pyrolysis in ambient air. Advanced Materials. 2011;**23**(16):1894

[62] Jeong S, Lee J-Y, Lee SS, Oh S-W, Lee HH, Seo Y-H, et al. Chemically improved high performance printed indium gallium zinc oxide thin-film transistors. Journal of Materials Chemistry. 2011;**21**(43):17066

[63] Navamathavan R, Nirmala R, Lee C. Effect of NH_3 plasma treatment on the device performance of ZnO based thin film transistors. Vacuum. 2011;**85**(9):904-907

[64] Kim E, Lee K, Kim D, Parsons GN, Park K, Ihm J, et al. SiNx charge trap nonvolatile memory based on ZnO thin film transistor prepared by atomic layer deposition. AIP Conf. Proc. 2011;**151**(2011):151-152

[65] Zhang L, Li J, Zhang XW, Yu DB, Jiang XY, Zhang ZL. Glass-substrate-based high performance ZnO-TFT by using a Ta2O5 insulator modified by thin SiO2 films. Physica Status Solidi (A) - Applications and Materials Science. 2010;**207**(8):1815-1819

[66] Bong H, Lee WH, Lee DY, Kim BJ, Cho JH, Cho K. High-mobility low-temperature ZnO transistors with low-voltage operation. Applied Physics Letters. 2010;**96**(19):192115

[67] Lu A, Sun J, Jiang J, Wan Q. Low-voltage transparent electric-double-layer ZnO-based thin-film transistors for portable transparent electronics. Applied Physics Letters. 2010;**96**(4):043114

[68] Zhang L, Li J, Zhang X. Low-voltage-drive and high output current ZnO thin-film transistors with sputtering SiO2 as gate insulator. Current Applied Physics. 2010;**10**(5):1306-1308

[69] Mourey DA, Member S, Zhao DA, Jackson TN. Self-aligned-gate ZnO TFT circuits. IEEE Electron Device Letters. 2010;**31**(4):326-328

[70] Bayraktaroglu B. Microwave ZnO thin-film transistors. Electron Device Letters. 2008;**29**(9):1024-1026

[71] Zhu J, Chen H, Saraf G, Duan Z. ZnO TFT devices built on glass substrates. Journal of Electronics. 2008;**37**(9):1237-1240

[72] Wei A, Pan L, Huang W. Recent progress in the ZnO nanostructure-based sensors. Materials Science & Engineering, B: Solid-State Materials for Advanced Technology. 2011;**176**(18):1409-1421

[73] Xia Y, Yang P, Sun Y, Wu Y, Mayers B, Gates B, et al. One-dimensional nanostructures: Synthesis, characterization, and applications. ChemInform. 2003;**34**(22)

[74] Hsu C, Tsai T. Fabrication of fully transparent indium-doped ZnO nanowire field-effect transistors on ITO/glass substrates. Journal of the Electrochemical Society. 2011;**158**(2):K20-K23

[75] Peng S, Su Y, Ji L. Semitransparent field-effect transistors based on ZnO nanowire networks. IEEE Electron Device Letters. 2011;**32**(4):533-535

[76] Kang CG, Kang JW, Lee SK, Lee SY, Cho CH, Hwang HJ, et al. Characteristics of CVD graphene nanoribbon formed by a ZnO nanowire hardmask. Nanotechnology. 2011;**22**(29):295201

[77] Wang Y, Sun XW, Zhao J, Goh GKL, Chen L, Liew L-L, et al. Comparison of the hydrothermal and VPT grown zno nanowire field effect transistors. International Journal of Nanoscience. 2010;**09**(4):317-320

[78] Park WI, Kim JS, Yi GC, Lee HJ. ZnO nanorod logic circuits. Advanced Materials. 2005;**17**(11):1393

[79] Ju S, Lee K, Janes DB, Dwivedi RC, Baffour-Awuah H, Wilkins R, et al. Proton radiation hardness of single-nanowire transistors using robust organic gate nanodielectrics. Applied Physics Letters. 2006;**89**(13):073510

[80] Heo Y, Tien L, Kwon Y. Depletion-mode ZnO nanowire field-effect transistor. Applied Physics. 2004;**85**(12):2274-2276

[81] Ng HT, Han J, Yamada T, Nguyen P, Chen YP, Meyyappan M. Single crystal nanowire vertical surround-gate field-effect transistor. Nano Letters. 2004;**4**(7):1247-1252

[82] Park JY, Yun YS, Hong YS, Oh H, Kim JJ, Kim SS. Synthesis, electrical and photoresponse properties of vertically well-aligned and epitaxial ZnO nanorods on GaN-buffered sapphire substrates. Applied Physics Letters. 2005;**87**(12):1-3

[83] Wang W, Xiong HD, Edelstein MD, Gundlach D, Suehle JS, Richter CA, et al. Low frequency noise characterizations of ZnO nanowire field effect transistors. Journal of Applied Physics. 2007;**101**(4)

[84] Kim H, Park J-H, Suh M, Real Ahn J, Ju S. Horizontally aligned ZnO nanowire transistors using patterned graphene thin films. Applied Physics Letters. 2012;**100**(6):063112

[85] Das S, Kim JH, Choi HS, Park YK, Hahn YB. Interfacial and electrical properties of solution processed p-TiO_2 in heterojunction devices. Electrochemistry Communications. 2011;**13**(4):350-354

[86] Noriega R, Rivnay J, Goris L, Kälblein D, Klauk H, Kern K, et al. Probing the electrical properties of highly-doped Al:ZnO nanowire ensembles. Journal of Applied Physics. 2010;**107**(7):074312

[87] Thévenot DR, Toth K, Durst RA, Wilson GS. Electrochemical biosensors: Recommended definitions and classification. Biosensors & Bioelectronics. 2001;**16**(1-2):121-131

[88] Roy S, Gao Z. Nanostructure-based electrical biosensors. Nano Today. 2009;**4**(4):318-334

[89] Jung J, Kim SJ, Lee KW, Yoon DH, Kim Y-G, Kwak HY, et al. Approaches to label-free flexible DNA biosensors using low-temperature solution-processed InZnO thin-film transistors. Biosensors & Bioelectronics. 2014;**55**:99-105

[90] Chen K, Li B, Chen Y. Silicon nanowire field-effect transistor-based biosensors for biomedical diagnosis and cellular recording investigation. Nano Today. 2011;**6**(2):131-154

[91] Yano M, Koike K, Ogata KI, Nogami T, Tanabe S, Sasa S. Zinc oxide-based biosensors. Physica Status Solidi (C) Current Topics in Solid State Physics. 2012;**9**(7):1570-1573

[92] Liu J, Goud J, Raj PM, Iyer M, Wang ZL, Tummala RR. Real-time protein detection using ZnO nanowire/thin film bio-sensor integrated with microfluidic system. In: Proceedings—Electronic Components and Technology Conference. 2008. pp. 1317-1322

[93] Liu X, Lin P, Yan X, Kang Z, Zhao Y, Lei Y, et al. Enzyme-coated single ZnO nanowire FET biosensor for detection of uric acid. Sensors and Actuators B: Chemical. 2013;**176**:22-27

[94] Mohd Azmi MA, Tehrani Z, Lewis RP, Walker KD, Jones DR, Daniels DR, et al. Highly sensitive covalently functionalised integrated silicon nanowire biosensor devices for detection of cancer risk biomarker. Biosensors & Bioelectronics. 2014;**52**:216-224

[95] Shen Y-C, Yang C-H, Chen S-W, Wu S-H, Yang T-L, Huang J-J. IGZO thin film transistor biosensors functionalized with ZnO nanorods and antibodies. Biosensors & Bioelectronics. 2014;**54**:306-310

[96] Choi A, Kim K, Jung H-I, Lee SY. ZnO nanowire biosensors for detection of biomolecular interactions in enhancement mode. Sensors and Actuators B: Chemical. 2010;**148**(2):577-582

[97] Cui Y, Wei Q, Park H, Lieber C. Nanowire nanosensors for highly sensitive and selective detection of biological and chemical species. Science (80-). 2001;**293**(5533):1289-1292

[98] Zheng G, Patolsky F, Cui Y, Wang WU, Lieber CM. Multiplexed electrical detection of cancer markers with nanowire sensor arrays. Nature Biotechnology. 2005;**23**(10):1294-1301

[99] Lu W, Xie P, Lieber CM. Nanowire transistor performance limits and applications. IEEE Transactions on Electron Devices. 2008;**55**(11):2859-2876

[100] Li Z, Chen Y, Li X, Kamins TI, Nauka K, Williams RS. Sequence-specific label-free DNA sensors based on silicon nanowires. Nano Letters. 2004;**4**(2):245-247

[101] Bunimovich YL, Shin YS, Yeo W-S, Amori M, Kwong G, Heath JR. Quantitative real-time measurements of DNA hybridization with alkylated nonoxidized silicon nanowires in electrolyte solution. Journal of the American Chemical Society. 2006;**128**(50):16323-16331

[102] Dorvel BR, Reddy B, Go J, Duarte Guevara C, Salm E, Alam MA, et al. Silicon nanowires with high-k hafnium oxide dielectrics for sensitive detection of small nucleic acid oligomers. ACS Nano. 2012;**6**(7):6150-6164

[103] Park I, Li Z, Li X, Pisano AP, Williams RS. Towards the silicon nanowire-based sensor for intracellular biochemical detection. Biosensors & Bioelectronics. 2007;**22**(9-10):2065-2070

[104] Tarasov A, Wipf M, Bedner K, Kurz J. True reference nanosensor realized with silicon nanowires, PubMed, Langmuir. May 2012;**28**(25):9899-9905. DOI: 10.1021/la301555r

[105] Zhang G-J, Zhang L, Huang MJ, Luo ZHH, Tay GKI, Lim E-JA, et al. Silicon nanowire biosensor for highly sensitive and rapid detection of dengue virus. Sensors and Actuators B: Chemical. 2010;**146**(1):138-144

[106] Stern E, Klemic J, Routenberg D. Label-free immunodetection with CMOS-compatible semiconducting nanowires. Nature. 2007;**445**(7127):519-522

[107] Lee M-H, Lee K-N, Jung S-W, Kim W-H, Shin K-S, Seong W-K. Quantitative measurements of C-reactive protein using silicon nanowire arrays. International Journal of Nanomedicine. 2008;**3**(1):117-124

[108] Chen S, Bomer JG, van der Wiel WG, Carlen ET, van den Berg A. Top-down fabrication of sub-30 nm monocrystalline silicon nanowires using conventional microfabrication. ACS Nano. 2009;**3**(11):3485-3492

[109] Sun K, Zeimpekis I, Lombardini M, Ditshego NMJ, Pearce SJ, Kiang KS, et al. Three-mask polysilicon thin-film transistor biosensor. IEEE Transactions on Electron Devices. 2014;**61**(6):2170-2176

[110] Zhang Y, Kang Z, Yan X, Liao Q. ZnO nanostructures in enzyme biosensors. Science China Materials. 2015;**58**(1):60-76

[111] Wei A, Sun XW, Wang JX, Lei Y, Cai XP, Li CM, et al. Enzymatic glucose biosensor based on ZnO nanorod array grown by hydrothermal decomposition. Applied Physics Letters. 2006;**89**(12):123902

[112] Yang K, She G-W, Wang H, Ou X-M, Zhang X-H, Lee C-S, et al. ZnO nanotube arrays as biosensors for glucose. Journal of Physical Chemistry C. 2009;**113**(47):20169-20172

[113] Aydoğdu G, Zeybek DK, Pekyardımcı Ş, Kılıç E. A novel amperometric biosensor based on ZnO

nanoparticles-modified carbon paste electrode for determination of glucose in human serum. Artificial Cells, Nanomedicine, and Biotechnology. 2013;**41**(5):332-338

[114] Fulati A, Ali SMU, Asif MH, Alvi NH, Willander M, Brännmark C, et al. An intracellular glucose biosensor based on nanoflake ZnO. Sensors and Actuators B: Chemical. 2010;**150**(2):673-680

[115] Yang Z, Zong X, Ye Z, Zhao B, Wang Q, Wang P. The application of complex multiple forklike ZnO nanostructures to rapid and ultrahigh sensitive hydrogen peroxide biosensors. Biomaterials. 2010;**31**(29):7534-7541

[116] Wang JX, Sun XW, Wei A, Lei Y, Cai XP, Li CM, et al. Zinc oxide nanocomb biosensor for glucose detection. Applied Physics Letters. 2006;**88**(23):233106

[117] Liu J, Guo C, Li CM, Li Y, Chi Q, Huang X, et al. Carbon-decorated ZnO nanowire array: A novel platform for direct electrochemistry of enzymes and biosensing applications. Electrochemistry Communications. 2009;**11**(1):202-205

[118] Yang C, Xu C, Wang X. ZnO/Cu nanocomposite: A platform for direct electrochemistry of enzymes and biosensing applications. Langmuir. 2012;**28**(9):4580-4585

[119] Wei Y, Li Y, Liu X, Xian Y, Shi G, Jin L. ZnO nanorods/Au hybrid nanocomposites for glucose biosensor. Biosensors & Bioelectronics. 2010;**26**(1):275-278

[120] Chu X, Zhu X, Dong Y, Chen T, Ye M, Sun W. An amperometric glucose biosensor based on the immobilization of glucose oxidase on the platinum electrode modified with NiO doped ZnO nanorods. Journal of Electroanalytical Chemistry. 2012;**676**:20-26

[121] Curreli M, Zhang R, Ishikawa FN, Chang HK, Cote RJ, Zhou C, et al. Real-time, label-free detection of biological entities using nanowire-based FETs. IEEE Transactions on Nanotechnology. 2008;**7**(6):651-667

[122] Wang WU, Chen C, Lin KH, Fang Y, Lieber CM. Labelfree detection of small-molecule–protein interactions by using nanowire nanosensors. Proceedings of the National Academy of Sciences of the United States of America. 2005;**102**:3208-3212

[123] Lei Y, Yan X, Luo N, Song Y, Zhang Y. ZnO nanotetrapod network as the adsorption layer for the improvement of glucose detection via multiterminal electron-exchange. Colloids and Surfaces A: Physicochemical and Engineering Aspects. 2010;**361**(1-3, 173):169

[124] Zhang F, Wang X, Ai S, Sun Z, Wan Q, Zhu Z, et al. Immobilization of uricase on ZnO nanorods for a reagentless uric acid biosensor. Analytica Chimica Acta. 2004;**519**(2):155-160

[125] Ali SMU, Ibupoto ZH, Kashif M, Hashim U, Willander M. A potentiometric indirect uric acid sensor based on ZnO nanoflakes and immobilized uricase. Sensors (Basel). 2012;**12**(3):2787-2797

[126] Jindal K, Tomar M, Gupta V. Inducing electrocatalytic functionality in ZnO thin film by N doping to realize a third generation uric acid biosensor. Biosensors & Bioelectronics. 2014;**55**:57-65

[127] Giri AK, Sinhamahapatra A, Prakash S, Chaudhari J, Shahi VK, Panda AB. Porous ZnO microtubes with excellent cholesterol sensing and catalytic properties. Journal of Materials Chemistry A. 2013;**1**(3):814-822

[128] Ahmad R, Tripathy N, Hahn Y-B. Wide linear-range detecting high

sensitivity cholesterol biosensors based on aspect-ratio controlled ZnO nanorods grown on silver electrodes. Sensors and Actuators B: Chemical. 2012;**169**:382-386

[129] Ahmad M, Pan C, Luo Z, Zhu J. A single ZnO nanofiber-based highly sensitive amperometric glucose biosensor. Journal of Physical Chemistry C. 2010;**114**(20):9308-9313

[130] Zhao ZW, Chen XJ, Tay BK, Chen JS, Han ZJ, Khor KA. A novel amperometric biosensor based on ZnO:Co nanoclusters for biosensing glucose. Biosensors & Bioelectronics. 2007;**23**(1):135-139

[131] Shukla SK, Deshpande SR, Shukla SK, Tiwari A. Fabrication of a tunable glucose biosensor based on zinc oxide/chitosan-graft-poly(vinyl alcohol) core-shell nanocomposite. Talanta. 2012;**99**:283-287

[132] Karuppiah C, Palanisamy S, Chen S-M, Veeramani V, Periakaruppan P. Direct electrochemistry of glucose oxidase and sensing glucose using a screen-printed carbon electrode modified with graphite nanosheets and zinc oxide nanoparticles. Microchimica Acta. 2014;**181**(15-16):1843-1850

[133] Wang Y-T, Yu L, Zhu Z-Q, Zhang J, Zhu J-Z, Fan C. Improved enzyme immobilization for enhanced bioelectrocatalytic activity of glucose sensor. Sensors and Actuators B: Chemical. 2009;**136**(2):332-337

[134] Palanisamy S, Cheemalapati S, Chen SM. Enzymatic glucose biosensor based on multiwalled carbon nanotubes-zinc oxide composite. International Journal of Electrochemical Science. 2012;**7**(9):8394-8407